

Effect of Plasma Area on Frequency of Monostatic Radar Cross Section Reduction

Jungje Ha¹ · Woongjae Shin¹ · Joo Hwan Lee¹ · Yuna Kim¹ · Doosoo Kim² ·
Yongshik Lee^{1,*} · Jong-Gwan Yook¹

Abstract

This work reports on the effect of plasma area on the frequency characteristics of the monostatic radar cross section (RCS) of a square metallic plate. A dielectric barrier discharge (DBD) plasma actuator consisting of 10 rings is proposed. The actuator is fabricated in three different configurations such that only three inner rings, seven inner rings, and all rings can be biased. By applying an 18-kV bias at 1 kHz, the three types of DBD actuators generate plasma with a total area of 16.96, 36.74, and 53.69 cm², respectively, in a ring or circular form. The experimental results reveal that when the DBD actuator is placed in front of a 20 mm × 20 cm conducting plate, the monostatic RCS is reduced by as much as 18.5 dB in the range of 9.41–11.65 GHz. Furthermore, by generating the plasma and changing the area, the frequency of maximum reduction in the monostatic RCS of the plate can be controlled. The frequency is reduced by nearly 20% in the X band when all rings are biased. Finally, an electromagnetic model of the plasma is obtained by comparing the experimental and full-wave simulated results.

Key Words: Dielectric-Barrier-Discharge Plasma, Frequency Tunable, Radar Cross Section Reduction, Surface Area of Plasma.

I. INTRODUCTION

On the battlefield, efficient surveillance radars use high-gain beams to obtain target information such as location and velocity. To counter the development of such radars, various stealth technologies have been developed to increase the survivability of weapon systems [1–3].

Electromagnetic stealth technology aims to reduce a target's radar cross section (RCS); the RCS describes how much electromagnetic power is scattered by the target. The most important factors that affect an object's RCS are its size, shape, and material. Thus, engineers have been developing planes with specific shapes that can redirect electromagnetic waves from

radars. For instance, the shape of the F-117 is optimized to minimize the amount of radar signals reflected back to the emitting radar [4]. However, stealth shaping techniques may have a limited effect because aerodynamic properties cannot be sacrificed.

Other popular methods for RCS reduction are radar-absorbing materials (RAM) and radar-absorbing structures (RAS) [5–8]. In these methods, lossy radar-absorbing materials are used to reduce the reflection of incident electromagnetic waves from the aircraft. However, these methods suffer from problems such as narrow band performance, high weight, and high fabrication and maintenance costs.

Recently, researchers have been investigating plasma technol-

Manuscript received June 26, 2017 ; Revised July 22, 2017 ; Accepted July 24, 2017. (ID No. 20170626-027J)

¹Department of Electrical and Electronic Engineering, Yonsei University, Seoul, Korea.

²Agency for Defense Development, Daejeon, Korea.

*Corresponding Author: Yongshik Lee (e-mail: yongshik.lee@yonsei.ac.kr)

This is an Open-Access article distributed under the terms of the Creative Commons Attribution Non-Commercial License (<http://creativecommons.org/licenses/by-nc/3.0>) which permits unrestricted non-commercial use, distribution, and reproduction in any medium, provided the original work is properly cited.

© Copyright The Korean Institute of Electromagnetic Engineering and Science. All Rights Reserved.

ogy as an alternative stealth method [9]; for example, one study investigated refraction, reflection, and absorption based on plasma surrounding a 2D cylinder. Popular methods for generating plasma include dielectric barrier discharge (DBD), plasma torch, and plasma jet [10]. Although all plasma-generating methods can be used to realize the low-observable characteristic, DBD is better than other plasma sources because it has the simplest structure and its size can be adjusted easily.

This work reports on the effect of plasma area on the frequency characteristics of the monostatic RCS of a square metallic plate. A DBD plasma actuator consisting of 10 rings is modified into three different configurations that have different plasma areas with connections of multiple electrodes. In this work, the three types of DBD actuators with different plasma areas are used by applying 18 kV bias at 1 kHz. For verification, the RCS is measured for the fabricated DBD in front of a 20-cm square metal plate. The experimental results reveal that the generated plasma area can be controlled to reduce the RCS, and also adjust the frequency of maximum reduction in the monostatic RCS of the plate. Furthermore, an electromagnetic model of the plasma is obtained by comparing the experimental and full-wave simulated results.

II. PROPOSED DBD PLASMA ACTUATOR AND ELECTROMAGNETIC MODELING OF PLASMA

Fig. 1 shows the proposed DBD plasma actuator. The actuator consists of concentric ring-shaped electrodes printed on both sides of a 200 mm × 200 mm FR-4 substrate with $\epsilon_r = 4.4$, $\tan \delta = 0.025$, 0.8-mm thickness, and 35- μm copper cladding. Ten rings are on the top layer and nine, on the other side. The outer radius of the largest ring is 88.5 mm, and the inner radius

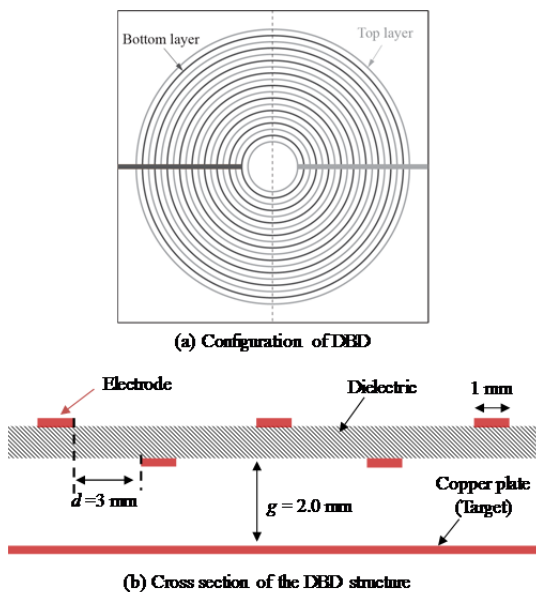


Fig. 1. Configuration of fabricated DBD plasma actuator.

of the smallest ring is 15.5 mm. The gap between two adjacent rings is $d = 3$ mm.

To generate plasma, an AC source is applied between the top and the bottom electrodes with a voltage that is higher than the breakdown voltage of the environment. The minimum breakdown voltage is described by Paschen's law [11, 12]:

$$V_b = \frac{B \times pd}{C + \ln(pd)} \quad (1)$$

where B and C are constants determined by the type of environmental gases, and p and d denote the pressure and distance between electrodes, respectively. In the atmosphere, the constants are $B = 365 \text{ V} \cdot \text{cm}^{-1} \cdot \text{Torr}^{-1}$ and $C = 1.18$ [10, 11]. From Eq. (1), the calculated minimum breakdown voltage is 8.9 kV. Based on the result, 18 kV is used for the stable generation of stable plasma, that is, glow discharge. Moreover, to prevent arc discharge between the plasma actuator and the nearby metallic object, namely, the copper plate, the two are separated by $g = 2.0$ mm.

Fig. 2 shows the measurement setup for the monostatic RCS of the 200 × 200 mm² square copper plate with the DBD actuator placed in front. An acrylic jig is used for accurate placement of the actuator and the copper target. The RCS measurement is performed in the 4–18 GHz range by using a pair of DRH-002G-018G double-ridged horn antennas and a 37247D vector network analyzer from Anritsu. Because the fabricated actuator comprises ring-shaped electrodes, the scattering characteristic is independent of the polarization of incident waves. In this work, only the incidence of a vertical-polarized wave is considered.

Fig. 3 shows the measured RCS for the fabricated DBD actuator in front of a 200 × 200 mm² copper plate with and

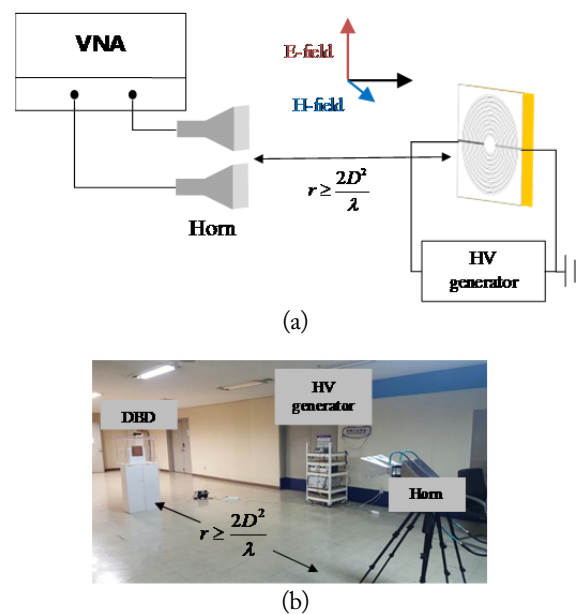


Fig. 2. Monostatic RCS measurement setup: (a) diagram, (b) photograph.

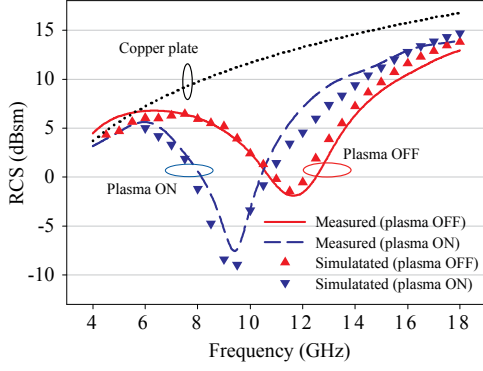


Fig. 3. Measured monostatic RCS of 200 mm × 200 mm copper plate with and without DBD actuator in front.

without plasma generation. Compared to both measured results, frequency shift can be achieved by plasma generation.

To obtain the equivalent model of the generated plasma, the electrical properties of the generated plasma are required. These can be derived from the dispersion relation of a wave in plasma. According to [12], this relation can be expressed as

$$k = \sqrt{\frac{\omega^2}{c^2} - \frac{\omega_p^2}{c^2 \left(1 - j \frac{\nu}{\omega}\right)}} \quad (2)$$

where k is a complex wavenumber; ω , the operating angular frequency; c , the speed of light; ν , the electron-neutral collision frequency; and ω_p , the plasma angular frequency, which can be calculated as follows [13]:

$$\omega_p = \sqrt{\frac{n_e e^2}{m_e \epsilon_0}} \cong 8\sqrt{n_e} \quad (3)$$

where n_e is the electron density; e , the charge of an electron; m_e , the electron mass; and ϵ_0 , the permittivity of free space. From Eq. (1), the effective permittivity of the plasma can be derived as

$$\epsilon = \epsilon_0 \left\{ 1 - \frac{\omega_p^2/\omega^2}{1 + \nu^2/\omega^2} - j \left(\frac{\nu}{\omega} \right) \left(\frac{\omega_p^2/\omega^2}{1 + \nu^2/\omega^2} \right) \right\} \quad (4)$$

Generally, the electron density at atmospheric pressure is $n_e = 10^{20}$ – 10^{21} m^{-3} [14]; then, the plasma frequency becomes 12.6–40.2 GHz. If ν/ω is small enough to be ignored, the effective permittivity of the plasma becomes an epsilon-negative medium, which provides electromagnetic characteristics similar to those of metals such as silver or gold [15]. In this work, the generated plasma is assumed to be a material with high conductivity ($\sigma \geq 1,000$).

In addition to the electromagnetic material characteristic, the geometric structure of the generated plasma is required. Fig. 4 shows the modelled structure of the generated plasma. The effective width W_{pi} and thickness T_{pi} of the generated plasma around the i^{th} ring are assumed to be inversely proportional to the radius of the i^{th} electrode ring. It is assumed that each ring

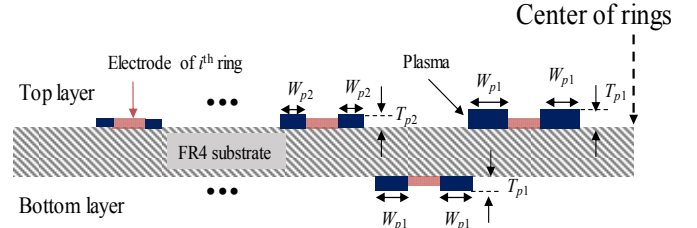


Fig. 4. Geometrically modelled structure of generated plasma.

Table 1. Physically modelled parameters for generated plasma

i^{th} ring	Top layer		Bottom layer	
	W_{pi} (μm)	T_{pi} (μm)	W_{pi} (μm)	T_{pi} (μm)
1 st	1,406	2,344	1,125	1,875
2 nd	937	1,563	803	1,339
3 rd	703	1,172	625	1,042
4 th	562	937	511	852
5 th	468	781	432	721
6 th	402	669	375	625
7 th	351	586	331	551
8 th	312	521	296	493
9 th	281	469	268	446
10 th	255	426	-	-

generates the same volume of plasma. By using a commercial software (ANSYS High Frequency Structure Simulator v10.0), the EM simulation is optimized; the physically modelled parameters for the generated plasma are summarized in Table 1.

The full-wave simulated RCS of the modeled plasma is plotted with the measured RCS in Fig. 3. Both results are in good agreement. Therefore, the simulated results indicate that plasma generation changes the scattering characteristic of an object by working as a high-conductivity material. These phenomena can also be observed in the ionosphere, where electromagnetic waves of 3–30 MHz are reflected [16].

III. EFFECT OF PLASMA AREA ON FREQUENCY OF MONOSTATIC RCS REDUCTION

As mentioned in the previous section, the generated plasma changes the scattering characteristic of the metal plate. In other words, different forms of generated plasma result in different scattering performances. Therefore, in this work, the minimum RCS frequency can be tuned by adjusting the area of the generated plasma. This can be achieved by switching the AC voltage between multiple rings. For verification, three cases are considered. In Type I, the DBD plasma actuator is constructed by connecting three inner rings on each side; Type II comprises seven inner rings on top and six rings on the other side; and Type III comprises all-connected rings on each side. Fig. 5 shows photographs of the different areas with the application of a high voltage of 18 kV.

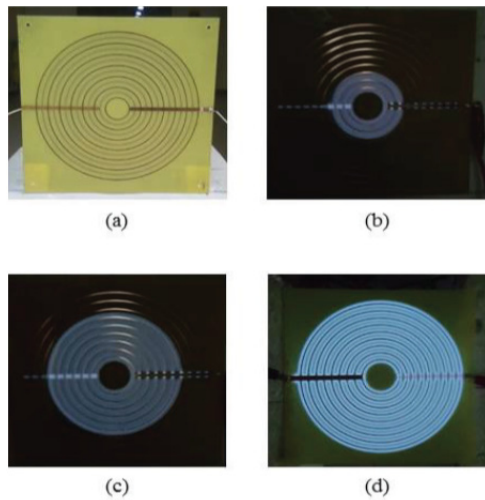


Fig. 5. Photographs of different models. (a) Plasma off, (b) Type I, (c) Type II, and (d) Type III.

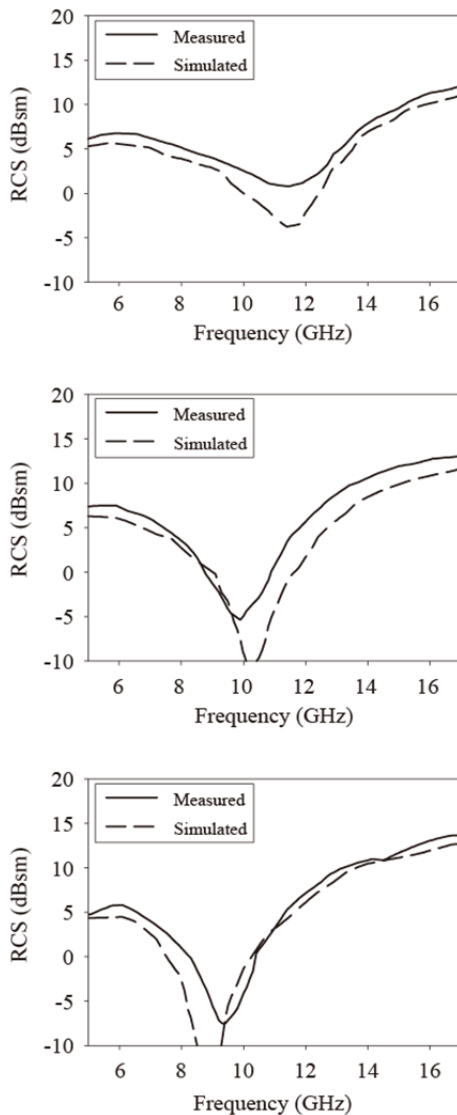


Fig. 6. Comparison with measurement results for all cases to shift monostatic RCS reduction frequency.

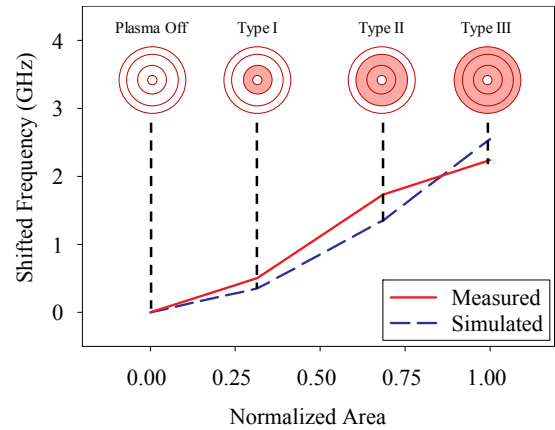


Fig. 7. Frequency shift with respect to normalized plasma area.

Fig. 6 shows the results of experiments with various areas of generated plasma. Although the measurement is conducted in a laboratory environment and not an anechoic chamber, we used time gating to neglect undesired waves reflected by the other obstacles; therefore, the measurement results are in good agreement with the simulation results, as shown in Fig. 6.

Fig. 6 shows that the frequency for minimum RCS is 11.65 GHz for the plasma off state. When applying a high voltage to the electrodes, the lowest RCS frequency becomes 11.25, 9.92, and 9.41 GHz for Types I, II, and III, respectively. Fig. 7 shows the amount of measured and simulated frequency shift depending on the generated plasma area. The amount of frequency shift increases with the plasma area, as shown in this figure.

IV. CONCLUSION

This work reports on the frequency effect of plasma area for monostatic RCS. To confirm the effect of plasma area, three types of DBD actuators are fabricated. The plasma areas are adjusted by the number of connected electrodes. For verification, the RCS of the fabricated DBD are simulated and measured. As a result, with an increase in the generated plasma area, the RCS is reduced as much as 18.5 dB and the frequency for minimum monostatic RCS changes from 11.65 to 9.41 GHz. Unlike plasma generated by previous DBD plasma actuators, the plasma generated in this work operates as a scattering material rather than an absorbing material. This phenomenon has not been observed in the microwave frequency regime. Therefore, future research could analyze the propagation characteristic in plasma. This can be extended to a very large structure by arranging the proposed DBD periodically.

This work was supported by the Low Observable Technology Research Center program of the Defense Acquisition Program Administration and Agency for Defense Development.

REFERENCES

- [1] Y. Sui, H. Gu, and C. Yang, "Reconfigurable stealth radome using active frequency selective surface technology," in *Proceedings of 2017 IEEE International Conference on Computational Electromagnetics (ICCEM)*, Kumamoto, Japan, 2017, pp. 273-275.
- [2] J. Pinto, J. C. G. Matthews, and G. C. Sarno, "Stealth technology for wind turbines," *IET Radar, Sonar and Navigation*, vol. 4, no. 1, pp. 126-133, 2010.
- [3] Y. C. Hou, W. J. Liao, C. C. Tsai, and S. H. Chen, "Planar multilayer structure for broadband broad-angle RCS reduction," *IEEE Transactions on Antennas and Propagation*, vol. 64, no. 5, pp. 1859-1866, 2016.
- [4] J. Pike, "F-117A Nighthawk," 2016; <https://fas.org/man/dod-101/sys/ac/f-117.htm>.
- [5] I. G. Lee, S. H. Yoon, J. S. Lee, and I. P. Hong, "Design of wideband radar absorbing material with improved optical transmittance by using printed metal-mesh," *Electronics Letters*, vol. 52, no. 7, pp. 555-557, 2016.
- [6] Y. Zhao, J. Liu, Z. Song, and X. Xi, "Microstructure design method for multineedle Whisker radar absorbing material," *IEEE Antennas and Wireless Propagation Letters*, vol. 15, pp. 1163-1166, 2016.
- [7] H. Singh and R. M. Jha, *Active Radar Cross Section Reduction: Theory and Applications*. Delhi: Cambridge University Press, 2015.
- [8] J. Lee and B. Lee, "Design of thin RC absorbers using a silver nanowire resistive screen," *Journal of Electromagnetic Engineering and Science*, vol. 16, no. 2, pp. 106-111, 2016.
- [9] L. X. Ma, H. Zhang, Z. Li, and C. X. Zhang, "Analysis on the stealth characteristic of two dimensional cylinder plasma envelopes," *Progress in Electromagnetics Research Letters*, vol. 13, pp. 83-92, 2010.
- [10] A. Schutze, J. Y. Jeong, S. E. Babayan, J. Park, G. S. Selwyn, and R. F. Hicks, "The atmospheric-pressure plasma jet: a review and comparison to other plasma sources," *IEEE Transactions on Plasma Science*, vol. 26, no. 6, pp. 1685-1694, 1988.
- [11] G. G. Raju and R. Hackam, "Note on Paschen law and the similarity theorem at the minimum breakdown voltage," *IEEE Transactions on Plasma Science*, vol. 2, no. 2, pp. 63-66, 1974.
- [12] A. A. Fridman and L. A. Kennedy, *Plasma Physics and Engineering*. Boca Raton, FL: CRC Press, 2004.
- [13] D. K. Cheng, *Field and Wave Electromagnetics*, 2nd ed. Reading, MA: Addison-Wesley, 1989.
- [14] L. Wei, S. Ying, and Q. Jinghui, "Experimental research on electromagnetic wave attenuation in plasma," in *Proceedings of the International Symposium on Antennas & Propagation (ISAP)*, Nanjing, China, 2013, pp. 1072-1074.
- [15] N. Engheta and R. W. Ziolkowski, *Metamaterials: Physics and Engineering Explorations*, New York, NY: John Wiley & Sons, 2006.
- [16] P. A. Fialer, "Field-aligned scattering from a heated region of the ionosphere: observations at HF and VHF," *Radio Science*, vol. 9, no. 11, pp. 923-940, 1974.

Jungje Ha



was born in Jinju, Gyeongnam, Korea, in 1985. He received the B.S., M.S., and Ph.D. degrees in Electrical Engineering from Yonsei University, Seoul, Korea, in 2009, 2011, and 2017, respectively. He received a Gold Award in the 2012 Qualcomm-Yonsei Innovation Award and the Grand Prize in the 2015 Creative Design Competition for Future Radio Wave. His current research interests include multiband planar circuits for microwave applications.

Woongjae Shin



was born in Seoul, Korea, in 1990. He received the B.S. and M.S. degrees in Electrical and Electronic Engineering from Chung-Ang University and Yonsei University, Seoul, Korea, in 2015 and 2017, respectively. His current research interests include low-observable applications based on plasma.

Joo Hwan Lee



was born in Seoul, Korea, in 1991. He received the B.S. degree in Information and Communication Engineering from Sejong University, Seoul, Korea, in 2016, and is currently working toward the M.S. degree in Electrical and Electronic Engineering at Yonsei University. His current research interests include low-observable applications based on plasma.

Yongshik Lee



was born in Seoul, Korea. He received the B.S. degree from Yonsei University, Seoul, Korea, in 1998, and the M.S. and Ph.D. degrees in Electrical Engineering from the University of Michigan at Ann Arbor in 2001 and 2004, respectively. In 2004, he was a postdoctoral research associate at Purdue University, West Lafayette, IN, USA. From 2004 to 2005, he was with EMAG Technologies, Inc., Ann Arbor, MI, USA as a Research Engineer. In September 2005, he joined Yonsei University, Seoul, Korea, where he is currently an Associate Professor. His current research interests include passive and active circuitry for microwave and millimeter-wave applications and electromagnetic metamaterials.

Yuna Kim



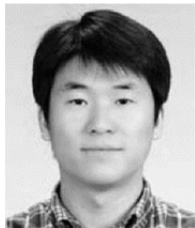
was born in Jinju, Korea, in 1988. She received the B.S. degree in Electrical and Electronic Engineering from Yonsei University, Seoul, Korea, in 2012, and is currently working toward the Ph.D. degree in Electrical and Electronic Engineering at Yonsei University. Her current research interest is analysis based on multi-physics including thermodynamics and electromagnetics. Recent research has focused on electric problems caused by high temperatures in circuit.

Jong-Gwan Yook



was born in Seoul, South Korea. He received the B.S. and M.S. degrees in Electronics Engineering from Yonsei University, Seoul, South Korea, in 1987 and 1989, respectively, and the Ph.D. degree from the University of Michigan, Ann Arbor, MI, USA, in 1996. Currently, he is a Professor with the School of Electrical and Electronic Engineering, Yonsei University, Seoul, South Korea. His main research interests are in the areas of theoretical/numerical electromagnetic modeling and characterization of microwave/millimeter-wave circuits and components, design of radio frequency integrated circuits and monolithic microwave integrated circuits, and analysis and optimization of high-frequency high-speed interconnects, including signal/power integrity, based on frequency as well as time-domain full-wave methods. Recently, his research team developed various biosensors, such as carbon nanotube RF biosensors for nanometer-sized antigen-antibody detection as well as remote wireless vital signal monitoring sensors.

Doosoo Kim



was born in Gwangju, Korea. He received the B.S. degree from Sogang University, Seoul, Korea, in 2001, and the M.S. degree in Electrical and Electronic Engineering from Postech, Pohang, Korea, in 2006. Currently, he works for the Agency for Defense Development (ADD), Daejeon, Korea, as a senior researcher. His current research interests include active phased array antenna systems and optimization algorithms.